Article

Alley cropping mitigates the impacts of climate change on wheat crop in a Mediterranean environment: a biophysical model based assessment

Supplementary Materials

Adjustments and completion of climatic series

Discrepancies in temperature between historical and field measured data were observed for our study site. These are probably related to the location of the experimental site in a lowland, where subsidence of cold air is occurring in winter, and overheating of air in summer, leading to more extreme temperatures than in the surroundings. Climatic data were adjusted to fit the local microclimate (**Figure S1**). Temperature values were adjusted as follows: the mean monthly difference (calculated for ten years from 2006 to 2015) between measured and projected (historical and *RCP 8.5*) min and max temperature were calculated and used to correct the same variables on the rest of the projected data series. Regarding the daily relative humidity (RH), its daily minimum and maximum values, needed in Hi-sAFe, are available in scenarios from Assessment Report 4 (AR4), but not in Assessment Report 5 (AR5), where only the mean RH is available. In order to obtain estimates of minimum and maximum RH for AR 5, we first fitted two linear models between daily precipitation, global radiation and the mean RH, and the minimum and maximum RH on AR4 data downloaded for the same site (R^2 = 0.90 for minumum RH, and R^2 = 0.86 for maximum RH) (**Table S1**). Then we applied these models to predict values of minimum and maximum RH in the temperature-adjusted AR 5 data set. Considering rainfall, differences of about nine percent were calculated between Hist and field measurements over 11 years (1995-2005) (measured: 982 mm $year^{-1}$, Hist: 1070 mm $year^{-1}$). However, given the high inter- and intra-annual variability of rainfall, the available data were not considered as sufficient to establish correction factors. Finally, projections of global radiation did not show significant discrepancies with measurements. Regarding carbon dioxide concentration, its mean annual values were obtained by a linear interpolation through historical and predicted values (RCP 8.5 in 1950 and 2100) [52] but without considering seasonal variations. The dynamics of the water table depth were reproduced by an empirical model calibrated for our experimental plots [28] and used to predict the depth of the water table as a function of rain events and potential evapotranspiration.

Table S1. Linear models for the prediction of maximum and minimum relative humidity.

p	Adj. R^2	term	estimate	SE	p value
Relative Humidity (minimum)	0.904	(Intercept)	-2.332	0.218	1.44E-26
		Relative Humidity	0.915	0.002	0
		Temperature (maximum)	-1.163	0.011	0
		Temperature (minimum)	1.376	0.012	0
		Precipitation (mm)	0.087	0.004	3.91E-100
		Global radiation	-0.172	0.006	2.14E-192
Relative Humidity (maximum)	0.856	(Intercept)	2.332	0.218	1.44E-26
		Relative Humidity	1.085	0.002	0
		Temperature (maximum)	1.163	0.011	0
		Temperature (minimum)	-1.376	0.012	0
		Precipitation (mm)	-0.087	0.004	3.91E-100
		Global radiation	0.172	0.006	2.14E-192

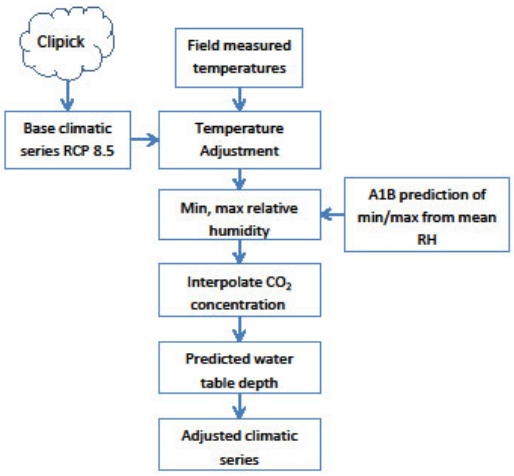

Figure S1. Procedure for microclimatic adjustments.

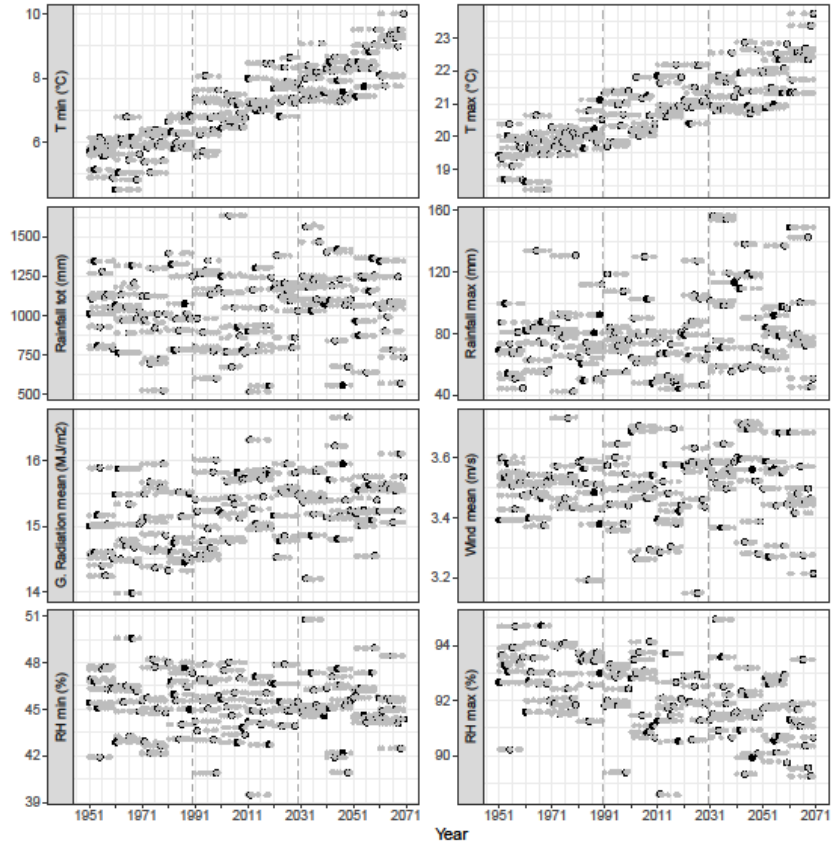

Figure S2. Pseudo-replicates of the climatic series. Mean of the minimum and maximum daily relative humidity and temperature; total annual and largest annual daily rainfall, mean daily mean wind speed and sum of global radiation. Black points indicate the original climatic series, grey points the pseudo-replicates. Vertical dashed lines separate time in periods corresponding to the simulated scenarios.

Principal Component Analysis on Climatic variables and stress indices

Here it is presented a Principal Component Analysis (PCA) on yearly climatic variables and stress indices (**Figure S3**). The first and second axes of the PCA on climate variables represented 69.5% of the total variability between years among Past, Present and Future scenarios. The first axis (44.71% of variability) opposed years with high global radiations and years with high relative humidity. The second axis (24.8% of variability) opposed years with high temperatures and rainfall to years with low temperatures and rainfall. Periods were relatively well separated on the PCA plane, with higher temperatures in the future. Unsurprisingly, when adding stress variables as supplementary variables, "cold" stresses (LowTempLUE, FrostFoliage and FrostPlantDensity) were negatively correlated with high temperatures, while high temperature stresses (TempGrainFilling, HighTempLUE) as well as SenecsenceWater and NitrogenLAIStress were positively correlated with high temperatures. Water stress was not correlated with any of the principal components.

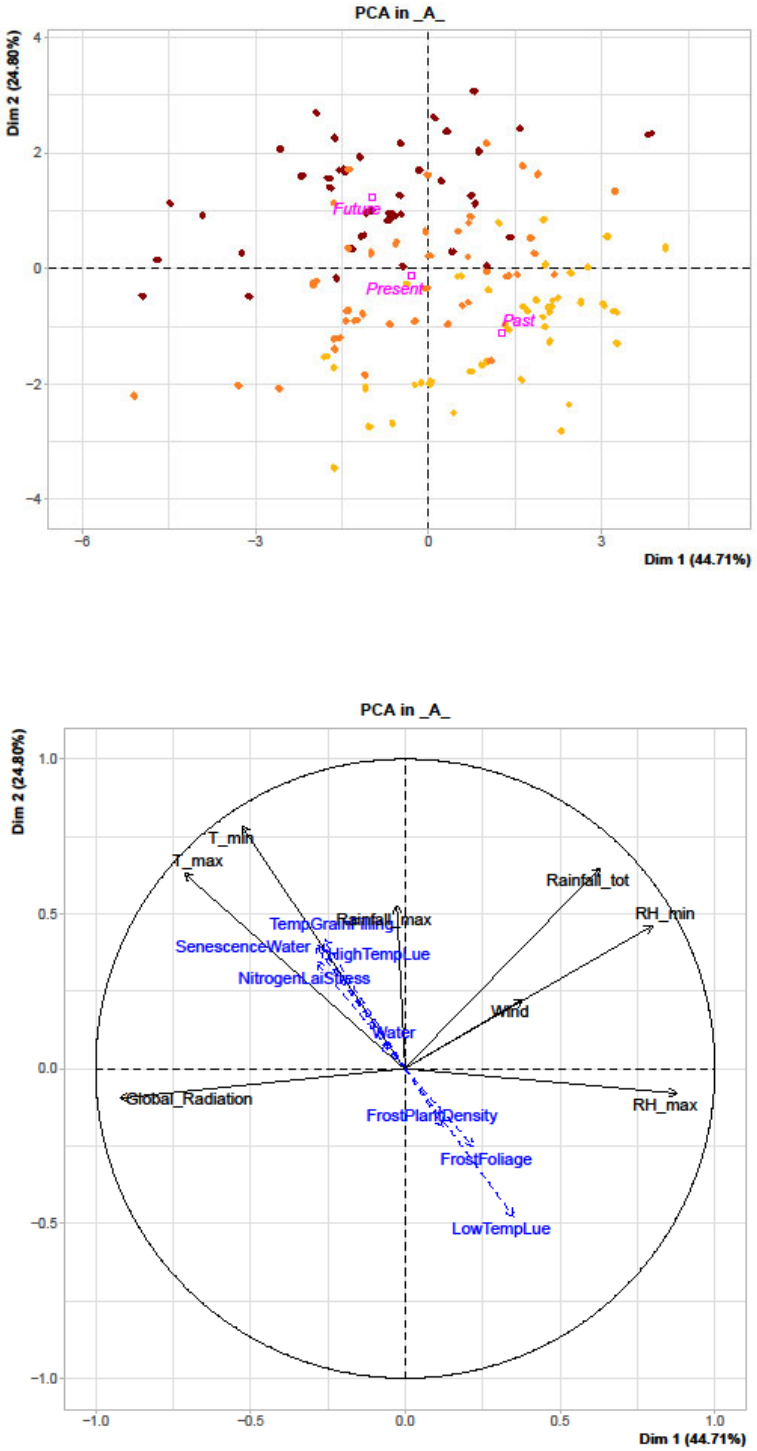

Figure S3. Principal component analysis of yearly climatic variables and stress indices in agriculture.

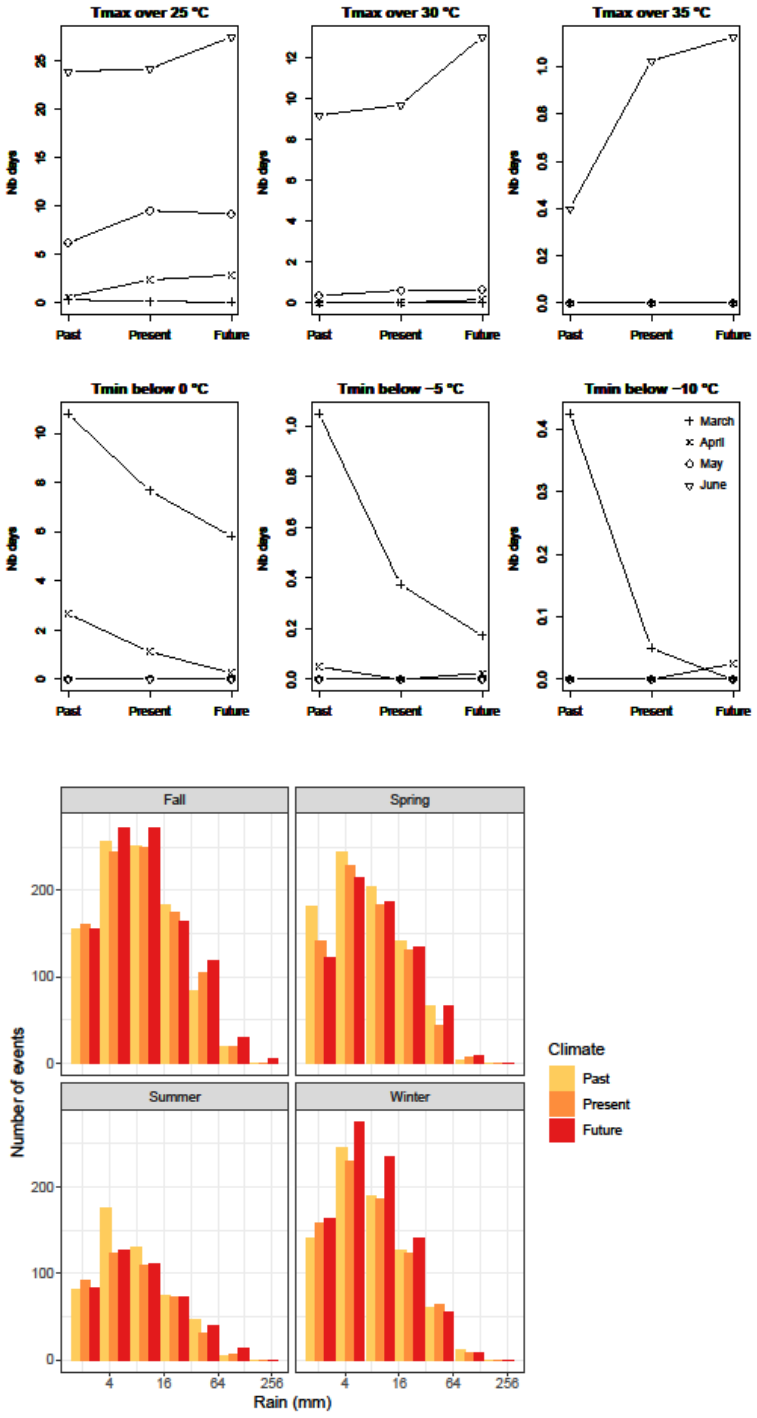

Figure S4. Extreme temperature and precipitation during the year and across *Past*, *Present* and *Future* scenarios. (Above) Number of days per year with maximum (Tmax) and minimum (Tmin) daily temperatures respectively above and below representative thresholds, for the months of March, April, May, and June. (Below) Number of rainfall events of a given intensity (values are log-transformed) divided per season and climatic scenario.

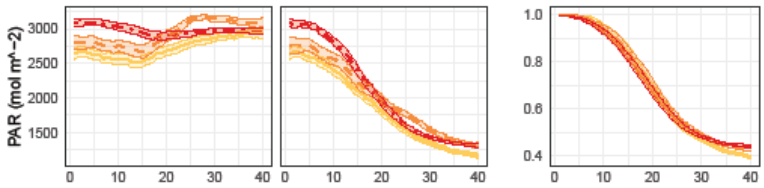

Figure S5. Mean daily PAR intercepted by the crop since tree plantation (A) in pure culture and alley cropping, and (B) relative values (AF/A), across scenarios. Each line represents the result of the application of a moving average window of 11 years across 11 pseudo-replicates of a climatic series. Vertical lines represent 95% confidence interval.

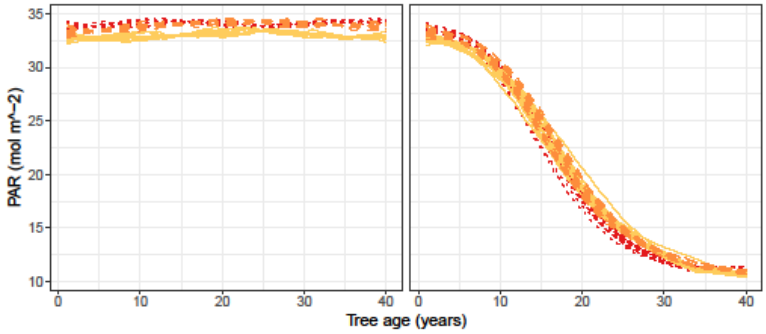

Figure S6. Mean daily PAR incident on the crop since tree plantation in pure culture and alley cropping across systems and scenarios. Individual lines represent repetitions, after averaging with a moving window of 11 years.

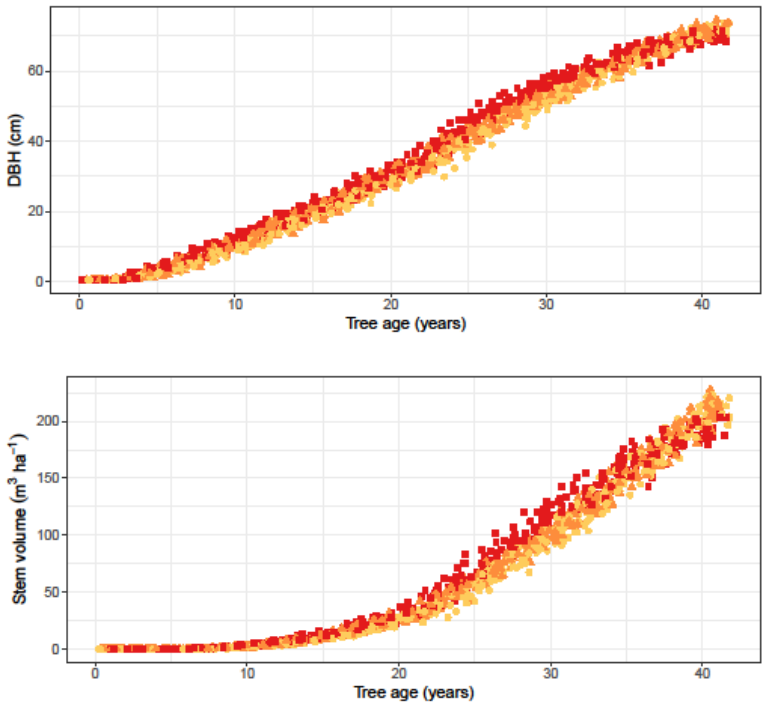

Figure S7. Simulated tree DBH (cm) (above) and stem volume ($m^3 ha^{-1}$) (at plot scale, below) in alley cropping systems over time.

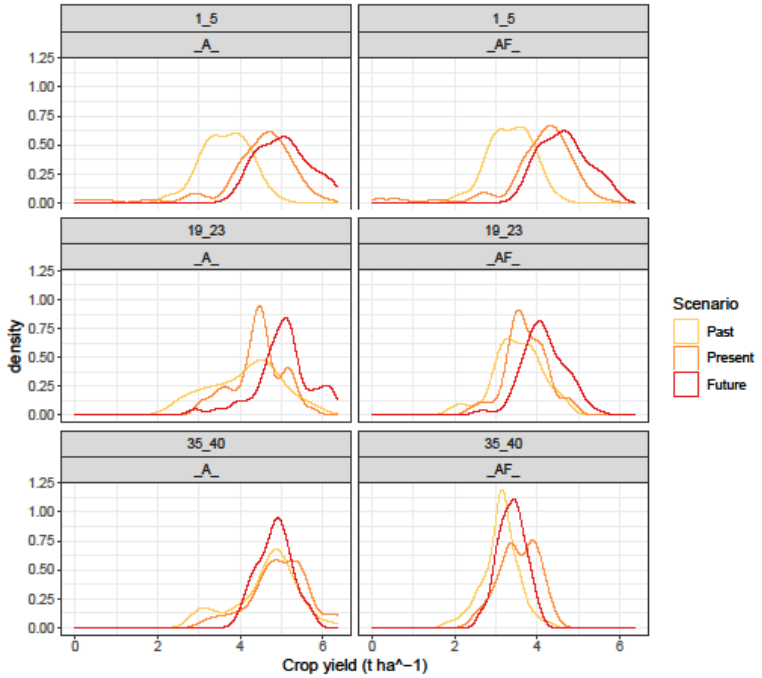

Figure S8. Yield distribution at plot scale, across scenarios and agricultural systems.

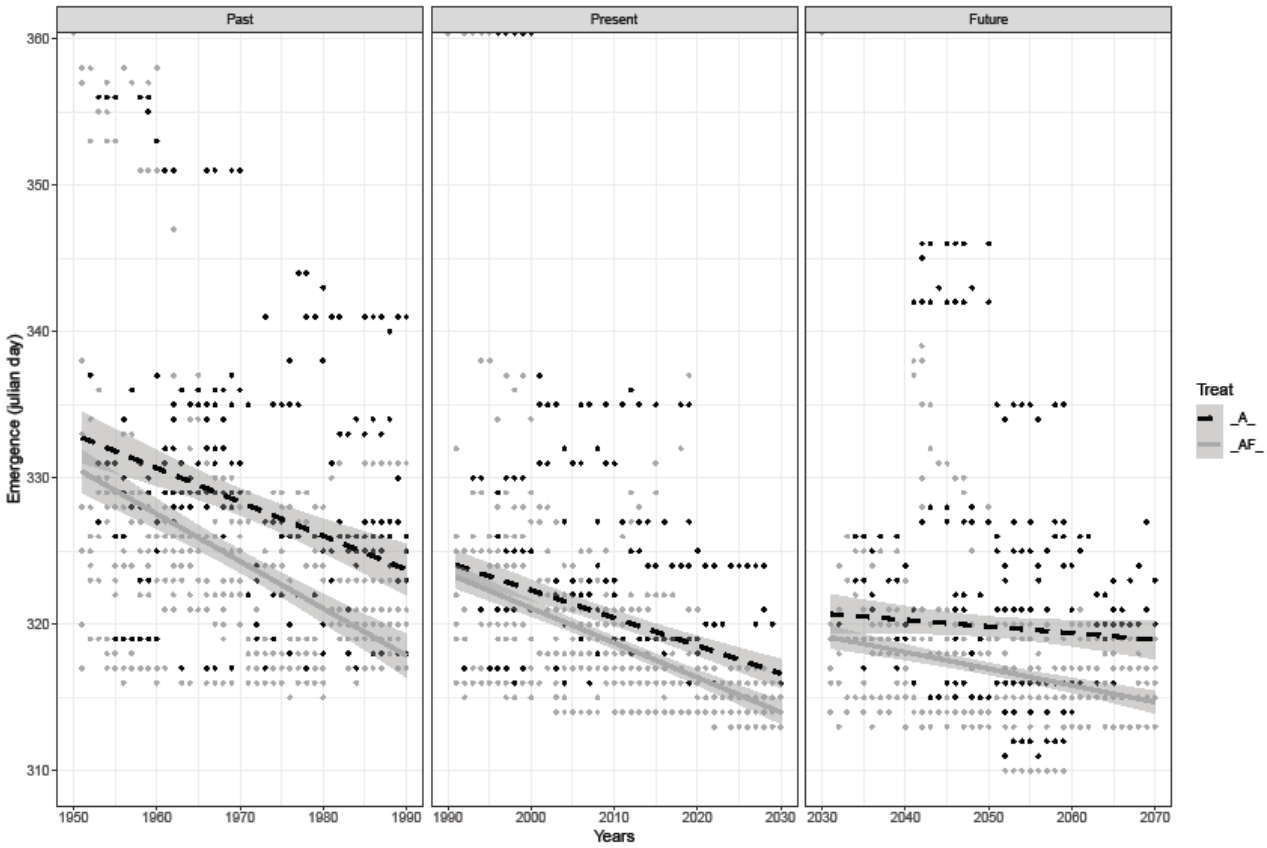

Figure S9. Variation in time of the day of plant emergence across scenarios and agricultural system (A dashed black line; AF solid grey line). A regression line with 95% confidence interval is also provided.

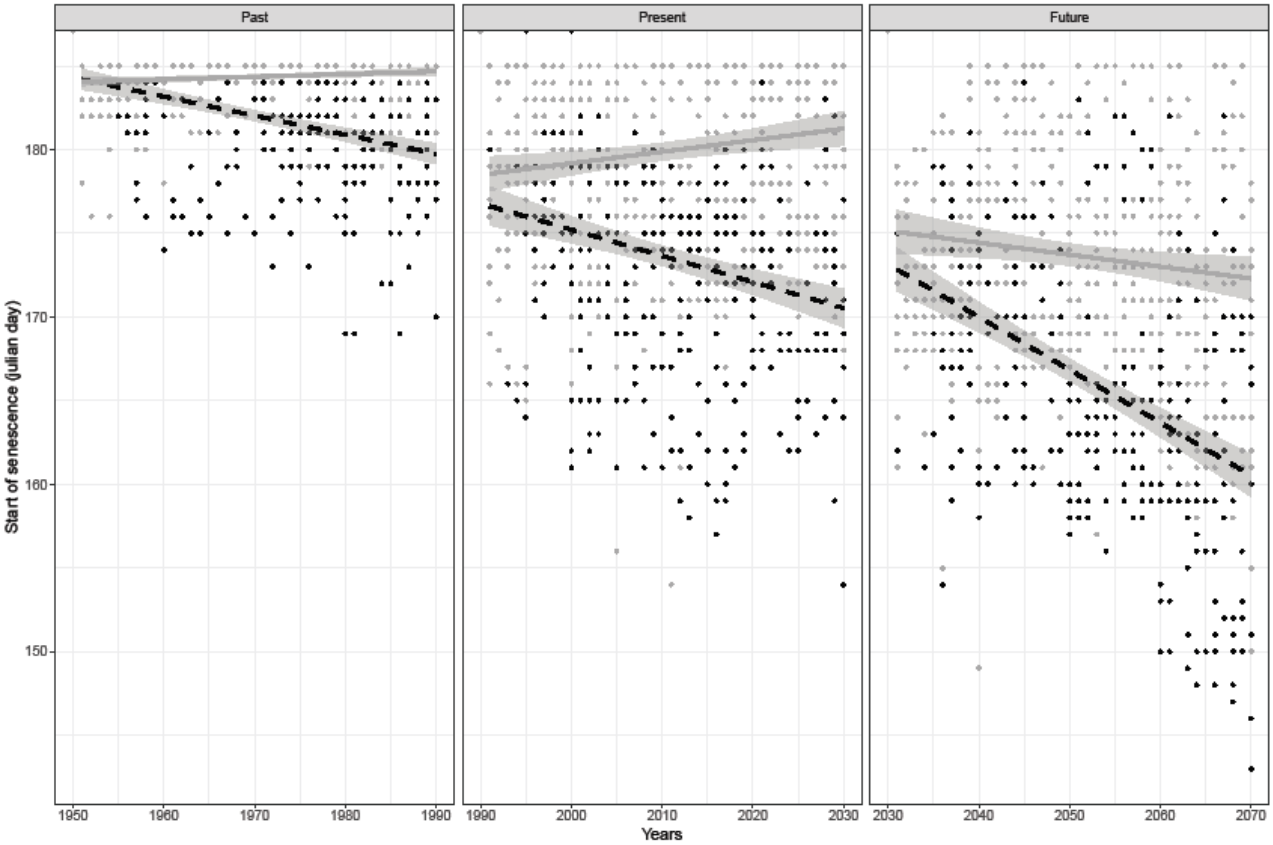

Figure S10. Variation in time of the day of start of plant senescence across scenarios and agricultural system (A dashed black line; AF solid grey line). A regression line with 95% confidence interval is also provided.

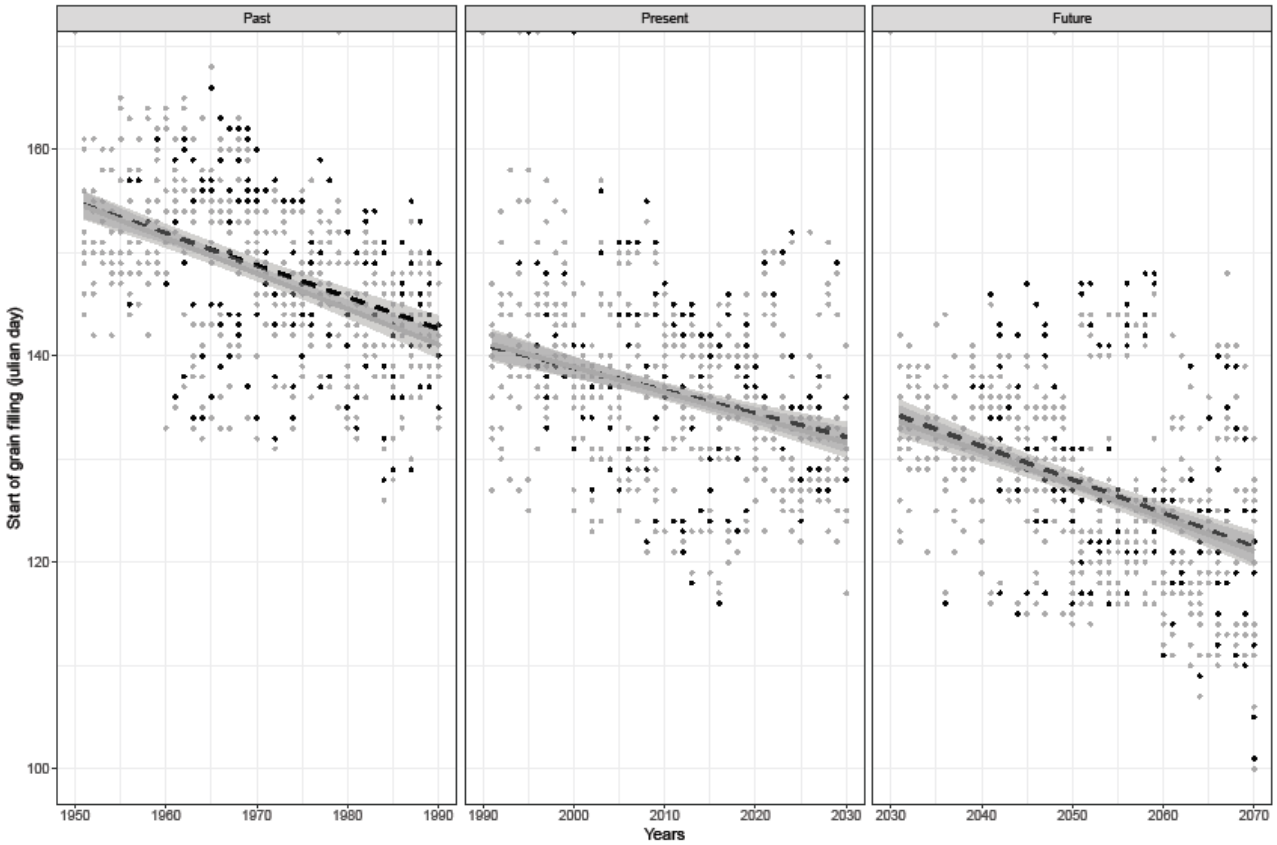

Figure S11. Variation in time of the day of start of grain filling across scenarios and agricultural system (A dashed black line; AF solid grey line). A regression line with 95% confidence interval is also provided.